

Suppressed-Moment 2-k Order in the Canonical Frustrated Antiferromagnet $\text{Gd}_2\text{Ti}_2\text{O}_7$ – Supplementary Information

Joseph A. M. Paddison,^{1,2,3,4,*} Georg Ehlers,⁵ Andrew B. Cairns,^{3,6}
Jason S. Gardner,¹ Oleg A. Petrenko,⁷ Nicholas P. Butch,⁸
Dmitry D. Khalyavin,⁴ Pascal Manuel,⁴ Henry E. Fischer,⁹
Haidong Zhou,^{10,11} Andrew L. Goodwin,³ J. Ross Stewart^{4,†}

¹Materials Science & Technology Division, Oak Ridge National Laboratory,
Oak Ridge, TN 37831, USA

²Churchill College, University of Cambridge, Storey's Way, Cambridge CB3 0DS, U.K.

³Inorganic Chemistry Laboratory, University of Oxford, South Parks Road, Oxford OX1 3QR, U.K.

⁴ISIS Neutron and Muon Source, Rutherford Appleton Laboratory, Didcot OX11 0QX, U.K.

⁵Neutron Technologies Division, Oak Ridge National Laboratory, Oak Ridge, TN 37831, USA

⁶Department of Materials, Imperial College London, Royal School of Mines, Exhibition Road,
London SW7 2AZ UK

⁷Department of Physics, University of Warwick, Coventry CV4 7AL, U.K.

⁸NIST Center for Neutron Research, National Institute of Standards and Technology,
Gaithersburg, MD 20899, USA

⁹Institut Laue-Langevin, 71 avenue des Martyrs, CS 20156, 38042 Grenoble Cédex 9, France

¹⁰Department of Physics and Astronomy, University of Tennessee, Knoxville, TN 37996, USA

¹¹National High Magnetic Field Laboratory, Florida State University, Tallahassee, FL 32310, USA

*To whom correspondence should be addressed; E-mail: paddisonja@ornl.gov.

†To whom correspondence should be addressed; E-mail: ross.stewart@stfc.ac.uk.

This manuscript has been authored by UT-Battelle, LLC under Contract No. DE-AC05-00OR22725 with the U.S. Department of Energy. The United States Government retains and the publisher, by accepting the article for publication, acknowledges that the United States Government retains a non-exclusive, paid-up, irrevocable, world-wide license to publish or reproduce the published form of this manuscript, or allow others to do so, for United States Government purposes. The Department of Energy will provide public access to these results of federally sponsored research in accordance with the DOE Public Access Plan (<http://energy.gov/downloads/doe-public-access-plan>).

(L_{1+}, L_{3-})	A	B
$E_g(L_{1+})$	+1.0	+1.0
$E_g(L_{3-})$	+0.175(8)	-0.175(8)

Supplementary Table 1: Refined values of magnetic distortion modes obtained for the (L_{1+}, L_{3-}) irrep pair. The magnitude of the $E_g(L_{1+})$ mode has been normalized to unity.

(L_{1+}, L_{3+})	C	D	E	F
$E_g(L_{1+})$	+1.0	+1.0	+1.0	+1.0
$A_{2g}(L_{3+})$	+0.167(9)	-0.167(9)	+0.344(9)	-0.344(9)
$E_{g1}(L_{3+})$	-0.163(9)	+0.163(9)	-0.090(9)	+0.090(9)
$E_{g2}(L_{3+})$	+0.206(11)	-0.206(11)	+0.173(11)	-0.173(11)

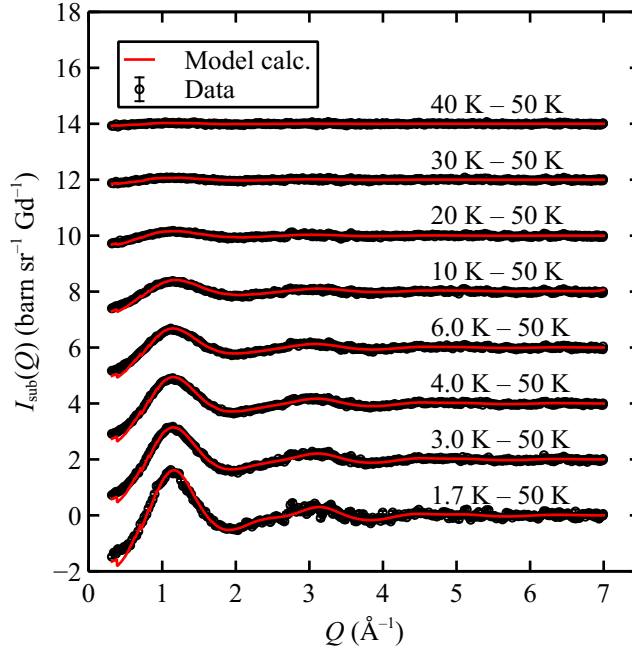
Supplementary Table 2: Refined values of magnetic distortion modes obtained for the (L_{1+}, L_{3+}) irrep pair. The magnitude of the $E_g(L_{1+})$ mode has been normalized to unity.

Irrep(s) No. of modes R_{wp}	L_{1+} 1 4.52(3)		(L_{1+}, L_{3-}) 2 4.23(3)		(L_{1+}, L_{3+}) 4 3.69(5)			
	Mag. SG	$\mu_{\text{ord}} (\mu_B)$	Mag. SG	$\mu_{\text{ord}} (\mu_B)$	Mag. SG	$\mu_{\text{ord}} (\mu_B)$		
1-k	$R_{\Gamma} \bar{3}m$	0.00, 6.55	$C_c m$ (A, B) $C_c 2$ (A, B)	1.97, 6.50, 6.50 1.97, 6.50, 6.50	$C_c 2/m$ (C) $C_c 2/m$ (D) $C_c 2/m$ (E) $C_c 2/m$ (F)	0.00, 5.44, 8.61 0.00, 7.63, 4.13 0.00, 5.95, 7.91 0.00, 7.52, 4.50		
	2-k	$C_a mcm$	4.63, 4.63, 8.02	$A_b m m 2$ (A, B) $A_b m a 2$ (A, B) $C_a 222_1$ (A, B) $C_a m c 2_1$ (A, B)	3.20, 5.98, 6.49, 6.49 3.20, 5.98, 4.59, 7.95 4.80, 4.59, 7.95 4.80, 4.59, 7.95	$C_a mcm$ (C) $C_a mcm$ (D) $C_a mcm$ (E) $C_a mcm$ (F)	6.07, 4.57, 6.22 2.93, 4.43, 9.82 5.57, 4.07, 7.39 3.19, 4.69, 9.54	
		3-k	$R_{\Gamma} \bar{3}m$	3.78, 6.55, 0.00, 7.56	$R_{\Gamma} 32$ (A, B)	3.92, 7.63, 5.36, 0.00, 7.51	$R_{\Gamma} \bar{3}m$ (C) $R_{\Gamma} \bar{3}m$ (D) $R_{\Gamma} \bar{3}m$ (E) $R_{\Gamma} \bar{3}m$ (F)	4.96, 7.28, 0.00, 4.77 2.40, 5.82, 0.00, 9.95 4.31, 7.55, 0.00, 5.22 2.86, 6.28, 0.00, 9.12
			4-k	$F_S 43m$	$I_c 4m 2$ (A)	0.98, 5.51, 7.04	$I_c 4m 2$ (C)	1.10, 7.51, 6.16
					$I_c \bar{4}m 2$ (B)	0.98, 7.47, 6.06	$I_c \bar{4}m 2$ (D)	1.10, 5.59, 7.11
			$I_c 4m 2$ (E)	1.10, 6.80, 6.56	$I_c 4m 2$ (E)	1.10, 6.80, 6.56		
			$I_c \bar{4}m 2$ (F)	1.10, 5.22, 7.25	$I_c \bar{4}m 2$ (F)	1.10, 5.22, 7.25		

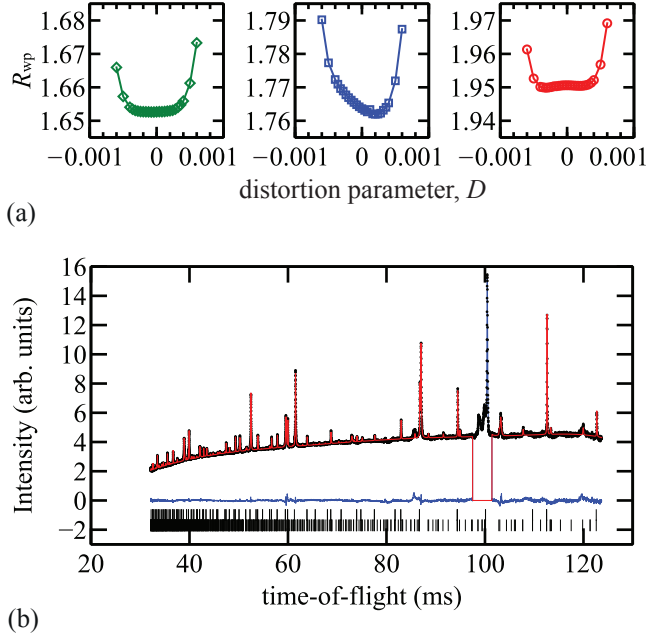
Supplementary Table 3: Magnetic space groups and magnitudes of ordered magnetic moments μ_{ord} for candidate magnetic structures of $\text{Gd}_2\text{Ti}_2\text{O}_7$. Statistical uncertainties in μ_{ord} are on the order of $0.1 \mu_B$. Where more than one magnetic space group and/or set of mode amplitudes yielded equally optimal fits to the experimental data, all possible values are given. Sets of mode amplitudes are labeled A–F and defined in Table 1 for the (L_{1+}, L_{3-}) irrep pair and in Table 2 for the (L_{1+}, L_{3+}) irrep pair. The 2 single-irrep structures and 8 two-irrep structures for which $\mu_{\text{ord}} \leq 7.0 \mu_B$ for all sites are shown in **bold**.

(x, y, z)	$[\mu_x, \mu_y, \mu_z]_{\mathbf{L}_{1+}}^{\text{Fit}}$	$[\mu_x, \mu_y, \mu_z]_{\mathbf{L}_{1+}, \mathbf{L}_{3+}}^{\text{Fit}}$	$[\mu_x, \mu_y, \mu_z]_{\mathbf{L}_{1+}, \mathbf{L}_{3+}}^{\text{Opt.}}$
$(\frac{1}{2}, \frac{1}{2}, \frac{1}{2})$	[3.28, 3.28, 0.00]	4.28, 4.28, 0.00	4.35, 3.41, 2.48
$(\frac{1}{2}, \frac{1}{4}, \frac{1}{4})$	[3.28, 3.28, 6.55]	3.48, 3.48, 3.77	3.68, 2.70, 4.20
$(\frac{3}{4}, 0, \frac{1}{4})$	[3.28, 3.28, 6.55]	3.48, 3.48, 3.77	3.68, 2.70, 4.20
$(\frac{3}{4}, \frac{3}{4}, \frac{1}{2})$	[3.28, 3.28, 0.00]	4.28, 4.28, 0.00	3.41, 4.35, 2.48
$(\frac{1}{4}, \frac{1}{2}, \frac{1}{4})$	[3.28, 3.28, 6.55]	3.48, 3.48, 3.77	3.68, 2.70, 4.20
$(0, \frac{3}{4}, \frac{1}{4})$	[3.28, 3.28, 6.55]	3.48, 3.48, 3.77	3.68, 2.70, 4.20
$(0, 0, \frac{1}{2})$	[3.28, 3.28, 0.00]	4.28, 4.28, 0.00	3.41, 4.35, 2.48
$(\frac{1}{4}, \frac{1}{4}, \frac{1}{2})$	[3.28, 3.28, 0.00]	4.28, 4.28, 0.00	4.35, 3.41, 2.48
$(0, \frac{1}{2}, 0)$	[3.28, 3.28, 0.00]	4.28, 4.28, 0.00	4.46, 3.59, 1.99
$(0, \frac{1}{4}, \frac{3}{4})$	[3.28, 3.28, 0.00]	3.22, 3.22, 0.00	3.22, 3.22, 0.00
$(\frac{1}{4}, 0, \frac{3}{4})$	[3.28, 3.28, 0.00]	3.22, 3.22, 0.00	3.22, 3.22, 0.00
$(\frac{1}{4}, \frac{3}{4}, 0)$	[3.28, 3.28, 0.00]	4.28, 4.28, 0.00	4.46, 3.59, 1.99
$(\frac{3}{4}, \frac{1}{2}, \frac{3}{4})$	[3.28, 3.28, 0.00]	3.22, 3.22, 0.00	3.22, 3.22, 0.00
$(\frac{1}{2}, \frac{3}{4}, \frac{3}{4})$	[3.28, 3.28, 0.00]	3.22, 3.22, 0.00	3.22, 3.22, 0.00
$(\frac{1}{2}, 0, 0)$	[3.28, 3.28, 0.00]	4.28, 4.28, 0.00	4.46, 3.59, 1.99
$(\frac{3}{4}, \frac{1}{4}, 0)$	[3.28, 3.28, 0.00]	4.28, 4.28, 0.00	4.46, 3.59, 1.99

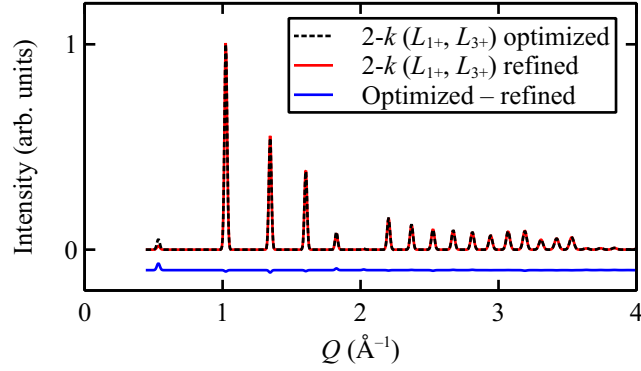
Supplementary Table 4: Ordered magnetic moment directions for 2-k magnetic structures. Magnetic moment components $[\mu_x, \mu_y, \mu_z]$ (in μ_B units) are referred to Cartesian basis vectors. Results are given for the crystallographic unit cell and magnetic moments in adjacent unit cells are related by $\mathbf{k} = (\frac{1}{2} \frac{1}{2} \frac{1}{2})$.



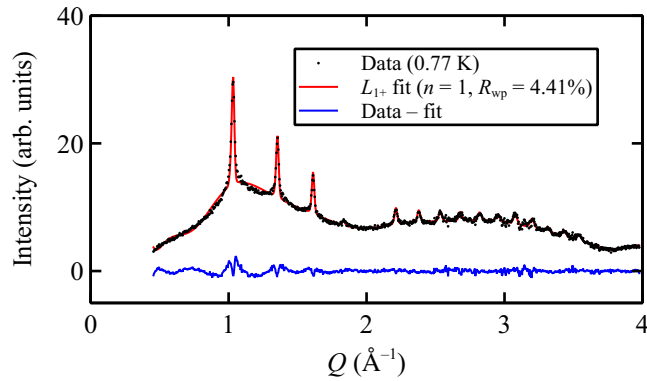
Supplementary Figure 1: Paramagnetic diffuse scattering data (black circles) and calculations for the model parameters given in the main text (red lines). Temperatures are indicated in the figure and successive temperatures are vertically shifted by 2 units for clarity. Data were collected on a powder sample containing natural Gd, using the D4 diffractometer at the ILL. Since the incident neutron wavelength of 0.5 \AA was shorter than the neutron resonances of absorbing Gd isotopes, the neutron absorption was weak enough to be accurately accounted for when normalizing the diffraction intensity to a V standard. Additionally, a high-temperature (50 K) measurement was subtracted from all data sets to remove background and nuclear scattering signals. Model calculations were performed using Monte Carlo simulations of Eq. (1) using the interaction parameters given in the main text, and following the methodology of Ref. (?). Model calculations have been vertically scaled by a factor of 0.85 and convolved with the D4 instrumental resolution function to match the experimental data.



Supplementary Figure 2: (a) Dependence of goodness-of-fit R_{wp} on the rhombohedral distortion parameter $D = c_h/\sqrt{6}a_h - 1$, where a_h and c_h are lattice parameters of the crystallographic unit cell in the hexagonal setting of space group $R\bar{3}m$. Rietveld refinements were performed in Topas 5 against powder neutron diffraction (PND) data measured on the HRPD instrument at ISIS at $T \approx 0.03$ K and $T = 1.1$ K. The sample was mounted in a Cu holder to which deuterated isopropyl alcohol (d-IPA) was added to improve thermal contact. Green diamonds in (a) show results for refinement of the nuclear phase to $T = 1.1$ K data, indicating that absence of a measurable lattice distortion in the paramagnetic phase. Blue squares in (a) show results for refinement of the magnetic+nuclear phase to $T = 0.03$ K data. Here, we refined two additional parameters to fit the magnetic phase: $\mu_{ord} = 6.7(1) \mu_B$, and a finite magnetic domain size $\xi_{domain} = 2.4(2) \times 10^3 \text{ \AA}$. The minimum R_{wp} is now obtained for very small but non-zero rhombohedral distortion $D = 0.00022(4)$ with lattice parameters $a_h = 7.19352(9) \text{ \AA}$ and $c_h = 17.6244(6) \text{ \AA}$. Notwithstanding the statistical significance of this result, no peak splitting indicative of a structural distortion is visible on careful inspection of the data (b). Red circles in (a) show results of refinement of the nuclear phase only to $T = 0.03$ K data, and indicate that the statistical sensitivity to the refined distortion is greatly reduced if the magnetic phase is not included in the fit. (b) High-resolution neutron diffraction pattern measured using HRPD at $T = 0.03$ K. Experimental data are shown as black circles, nuclear+magnetic Rietveld fit as a red line, and data-fit as a blue line. Time-of-flight is related to d -spacing here as $\text{TOF}(\mu\text{s}) = 0.27394 + 48213.48769 d - 5.50739 d^2$. The upper line of tick marks indicates the positions of nuclear Bragg peaks and the lower line of tick marks indicates the positions of magnetic Bragg peaks. Cu and V peaks from sample environment were also included by Pawley refinement. The region around 100 ms was excluded as it contains a large background contribution from d-IPA that could not be robustly refined.



Supplementary Figure 3: Calculated magnetic diffraction patterns for the optimized (L_{1+} , L_{3+}) structure (black dashed line) and refined (L_{1+} , L_{3+}) structure (solid red line) given in Table 4. The difference curve is shown as a blue line. The two structures have very similar diffraction patterns.



Supplementary Figure 4: Experimental powder neutron-diffraction data collected on the D20 diffractometer at the ILL ($\lambda = 2.42 \text{ \AA}$) in the intermediate-temperature phase (0.77 K) and Rietveld fits for the L_{1+} irrep. Experimental data are shown as black points, fits as red lines, and data–fit as blue lines. The number of free parameters (magnetic distortion modes) n and the goodness-of-fit metric R_{wp} is shown. The refined value of the ordered magnetic moment for a 1-k or 4-k magnetic structure is $2.65(3) \mu_{\text{B}}$ per Gd at 0.77 K.